Available online at www.sciencedirect.com

SciVerse ScienceDirect

Advances in Space Research 51 (2013) 754–771

ADVANCES IN SPACE RESEARCH (a COSPAR publication)

www.elsevier.com/locate/asr

Multi-station observation of ionospheric irregularities over South Africa during strong geomagnetic storms

Emirant Bertillas Amabayo *, J. Cilliers Pierre

South African National Space Agency (SANSA) Space Science, P.O. Box 32, Hermanus 7200, South Africa

Received 25 June 2012; received in revised form 18 October 2012; accepted 21 October 2012
Available online 30 October 2012

Abstract

This paper presents results pertaining to the response of the mid-latitude ionosphere to strong geomagnetic storms that occurred from 31 March to 02 April 2001 and 07–09 September 2002. The results are based on (i) Global Positioning Systems (GPSs) derived total electron content (TEC) variations accompanying the storm, (ii) ionosonde measurements of the ionospheric electrodynamic response towards the storms and (iii) effect of storm induced travelling ionospheric disturbances (TIDs) on GPS derived TEC. Ionospheric data comprising of ionospheric TEC obtained from GPS measurements, ionograms, solar wind data obtained from Advanced Composition Explorer (ACE) and magnetic data from ground based magnetometers were used in this study. Storm induced features in vertical TEC (*VTEC*) have been obtained and compared with the mean *VTEC* of quiet days. The response of the mid-latitude ionosphere during the two storm periods examined may be characterised in terms of increased or decreased level of *VTEC*, wave-like structures in *VTEC* perturbation and sudden enhancement in hmF2 and h′F. The study reveals both positive and negative ionospheric storm effects on the ionosphere over South Africa during the two strong storm conditions. These ionospheric features have been mainly attributed to the travelling ionospheric disturbances (TIDs) as the driving mechanism for the irregularities causing the perturbations observed. TEC perturbations due to the irregularities encountered by the satellites were observed on satellites with pseudo random numbers (PRNs) 15, 17, 18 and 23 between 17:00 and 23:00 UT on 07 September 2002.

Keywords: Mid-latitude spread F; TEC variability; TEC perturbation; Ionospheric irregularities

1. Introduction

Solar activity variations are known to occur as a result of the ionosphere's response to increased sunspot activity or sporadic phenomena like Coronal Mass Ejection (CMEs), solar flares or X-ray flares. All these processes raise radiation levels resulting in increased plasma densities in the ionosphere. A CME is a large-scale disturbance propagating from the Sun's outer corona into the solar wind and is mostly associated with solar flares. Such sporadic phenomena often causes geomagnetic storm as they propagate towards the Earth. During geomagnetic storms, ionospheric disturbance sources such as enhanced equatorward winds, composition changes, and electric field penetrations are often observed at middle and lower latitudes. These sources are believed to be closely related to substorm activities at high latitudes, meanwhile electric field penetration or over shielding processes are associated with ring current variations (Pi et al., 1993). According to Kintner et al. (2007), mechanical, electrical and chemically interrelated causal mechanisms are available for explaining storm related dynamics. One of these is the transitionary electric fields from the solar wind that propagates into the inner magnetosphere to the mid-latitude and low latitude over a 1–2 h period. This phenomenon leads to ionospheric uplift due to enhanced E×B drift and increased TEC during the day (Fejer and Scherliess, 1998). The mechanical process occurs when the high latitude thermosphere is heated up by auroral processes (Joule heating).

* Corresponding author. Tel.: +27 (28) 312 1196; fax: +27 (28) 312 2039.
E-mail addresses: emirant.amabayo@gmail.com (E.B. Amabayo), pjcilliers@hmo.ac.za (J. Cilliers Pierre).

0273-1177/$36.00 © 2012 COSPAR. Published by Elsevier Ltd. All rights reserved.
http://dx.doi.org/10.1016/j.asr.2012.10.015

This drives thermospheric winds equatorward via the mid-latitude, which also lifts the ionosphere. Accompanying the thermospheric winds are composition changes in the thermosphere which chemically remove plasma. Therefore, a good knowledge of the competing electric fields as well as thermospheric dynamics and composition changes is required to explain mid-latitude ionospheric storms effects (Kintner et al., 2007).

The study of low latitude ionospheric electric fields and currents by Fejer (1998) using incoherent scatter radar measurements from Arecibo (18°N, 67°W, dip latitude 30°N) and Jicamarca (11.9°S, 76.8°W, dip latitude 1°N) showed that ionospheric parameters are often strongly disturbed during periods of enhanced geomagnetic activity. Their results show that perturbations are consistent with the occurrence of strong prompt penetration electric fields reaching the magnetic equator, and can last for several hours after geomagnetic quieting. Two types of disturbance electric fields (i.e. prompt penetration zonal and disturbance dynamo electric fields) were identified by Kumar and Singh (1982) at the low latitudes. The prompt penetration electric fields are produced both during the southward turning of the interplanetary magnetic field (IMF) component (Bz) and during the terminating phase of a storm when IMF (Bz) turns northward. Disturbance dynamo electric fields are produced due to increases in radiation and consequent Joule heating of the high latitude plasma (Blanc and Richmond, 1980). Kumar and Singh (1982) add that this additional heating may launch equatorward winds, which in turn generate disturbance dynamo fields.

The dispersive ionospheric medium affects GPS signals in a number of ways as they pass from the satellites to the ground receivers. One of the significant effects is that the GPS signals traversing the ionosphere experiences an additional delay proportional to the TEC. TEC between a dual frequency receiver and the GPS satellites is calculated from L1 and L2 carrier signals and codes transmitted simultaneously by the GPS satellites. Since the frequencies that are used in the GPS system are sufficiently high, the signals are less affected by the ionospheric absorption and the Earth's magnetic field, both in the short-term and long-term changes in the ionospheric structure (Kumar and Singh, 1982). TEC is defined as the total number of free electrons in a cylinder of 1 m^2 cross-section between a receiver and a satellite along the line of sight. However, sudden variations in TEC degrade the phase and amplitude of the received GPS signal. The degradation of the signals is an impediment to the trans-ionospheric communication and navigation. In the mid-latitude zone, signal degradation due to large variations in TEC are mostly associated with geomagnetic storms. These storm induced TEC variations introduce additional range errors in the mid-latitudes. Ionospheric response to geomagnetic storms in terms of TEC varies, depending on the geographic location of the receiver, and the strength and local time of occurrence of the storm (Dashora et al., 2005) [references here in].

Therefore, a complete understanding of the processes that lead to ionospheric TEC variations during each storm in real time is needed to account for the errors in GPS navigation. The effect of a geomagnetic storm on the derived GPS TEC at low latitudes at Varanasi (geomagnetic lat. 14.92°N, geomagnetic long. 154°E) during the period May 2007 to April 2008 was investigated by Kumar and Singh (2010). This study found that TEC increased during the main phase of the storm during March 2008, while in the case of the November 2007 storm, TEC decreased during the main phase of the storm, but increased during the recovery phase of the storm. The ionospheric TEC at mid-latitudes examined by researchers such as e.g., Essex et al. (1972) and Prölss et al. (1991) was shown to have a major response to geomagnetic storms and substorms. The response is mainly attributed to combined effect of dynamical and chemical processes. Thermospheric circulation variations due to Joule heating and energetic particle precipitations in the auroral zone, and electric field perturbations are thought to be the major sources of the dynamical disturbances in the middle and lower latitude ionosphere (Fuller-Rowell et al., 1981). During substorms travelling atmospheric disturbances (TADs), also triggered by high-latitude Joule heating and particle precipitations, can cause TIDs on a global scale (e.g., Prölss and Jung, 1978; Fuller-Rowell et al., 1981; Prölss et al., 1991).

1.1. Data and methods

The ionospheric data used in this study was obtained from three ionosondes and six GPS receivers as shown in Table 1. TEC is a key parameter in describing the ionosphere and the correct ionospheric effects which lowers Global Navigation Satellite System positioning (GNSS) accuracy. The influence of the ionosphere on GNSS measurements depends on the GNSS wave frequency and on the TEC. The received codes from GPS satellites at the two frequencies ($f1 = 1575.42$ MHz and $f2 = 1227.60$ MHz) often show a differential bias due to different hardware paths inside the transmitter. The phases also experience offsets as a result of unknown carrier phase

Table 1
Geographical coordinates of the ionosonde and GPS receivers used in this study.

Station	Station code	Longitude (°E)	Latitude (°S)
Ionosonde stations			
Grahamstown	GR13L	26.50	33.32
Louisvale	LV12P	21.24	28.51
Madimbo	MU12K	30.88	22.38
GPS stations			
East London	ELDN	27.83	33.04
HartRAO	HRAO	27.69	25.89
Pretoria	PRET	28.28	25.73
Springbok	SBOK	17.88	29.67
Sutherland	SUTH	20.81	32.38
Ulundi	ULDI	31.42	28.29

ambiguities and differential equipment phase delays (Wanninger, 1993). Satellites are mostly observed along oblique signal paths which pierce the ionosphere at an assumed ionospheric shell height commonly known as the ionospheric pierce point (IPP). The IPP corresponds to the height typically associated with the peak electron density in the ionosphere (~350 km for this study).

A radio signal propagating through the ionosphere experiences a group delay and phase advance due to the ionosphere's dispersive nature. This delay or advance is proportional to the TEC along the signal path and inversely proportional to the square of the carrier frequency (f) and is given, to first order, by Hoffmann-Wellenhof et al. (1992). TEC is determined from GPS measurements by combining the dual frequency carrier phase and code-delay along the satellite-receiver line of sight. The pseudorange is increased by the ionospheric effect and is given in units of length by Hoffmann-Wellenhof et al. (1992). Code-based TEC (TEC_P) is noisier than phase-based TEC (TEC_L), largely due to multipath, but the latter suffers an unknown integer ambiguity offset and is subject to cycle slips associated with rapid ionospheric scintillations. Code-and carrier phase-based TEC are calculated from the difference between the two pseudo ranges and carrier phases as in Opperman et al. (2007). Corrected TEC_L is obtained from TEC_P by use of a levelling process by which continuous sections of TEC_L are adjusted to the mean of corresponding sections of TEC_P. The resultant product is the GPS-derived slant TEC (STEC) along the signal path between satellite and receiver (Opperman et al., 2007). STEC calculated along oblique signal paths are mapped to vertical TEC ($VTEC$) by means of a single layer model. STEC mathematically is defined as:

$$\mathrm{STEC} = \int_R^S N_e ds, \tag{1}$$

where TEC is measured in TEC Units (TECU) with 1 TECU $= 10^{16}$ electrons per m^2, R and S stand for the receiver and satellite positions respectively in km. The line integral is assumed to include all the electrons in a column with a cross-section of 1 m^2 and extending from receiver to satellite. The single layer mapping function takes the form below.

$$\mathrm{VTEC} = \mathrm{STEC} \times \sqrt{1 - \left(\frac{R_E \times sin(z_o)}{R_E + h_m}\right)^2}, \tag{2}$$

where R_E and h_m are the mean radius of the earth and height of the ionosphere respectively, both measured in km, and z_o is the zenith angle (in degrees or radians) at the observation site. For a known satellite position, z_o can then be calculated and the approximate coordinates of the IPP can be determined.

The Adjusted Spherical Harmonic (ASHA) analysis model was used in this study and uses spherical harmonics filter to estimate TEC (Opperman et al., 2007) as:

$$\mathrm{TEC}(\lambda,\phi) = \sum_{n=0}^{N}\sum_{m=0}^{n} \overline{P}_{nm}[cos(\phi)]\{a_{nm} sin(m\lambda) + b_{nm} cos(m\lambda)\}, \tag{3}$$

where λ is ionospheric pierce point (IPP), Sun fixed longitude $\in [0°; 360°]$; $\phi =$ IPP co-latitude $\in [0°; 180°]$; $\overline{P}_{nm}$ is equal to normalised associated Legendre function of degree n and order m. $a_{nm}, b_{nm} \equiv$ are the desired Spherical Harmonic Model (SHM) coefficients and n, m are the degree and order of SHM expansion.

Further details of the ASHA model based derivation of TEC can be found in Opperman et al. (2007). The derived TEC was then further processed to obtained the perturbations in the $VTEC$. The data for each GPS receiver for a number of quiet days before and after the event was used to calculate the background TEC (mean $VTEC$) of the data points for every 30 seconds in order to smooth out the quiet day data. The quiet day mean $VTEC$ ($\overline{VTEC}$) was then used to compute the $VTEC$ perturbation using the expression below.

$$VTEC \text{ perturbation} = VTEC_{observed} - \overline{VTEC}.$$

The diurnal and latitude variations of the $VTEC$ was also examined in this study. This was done by processing data for all the available receivers together and interpolating using the coordinates of a reference (a central) receiver station to obtain the SHM coefficients. The TEC calculated using the SHM coefficients is then used to investigate the diurnal and latitude pattern of TEC over the South African region.

2. Results and discussion

In this paper, SF events during high solar activity period (2001–2003) were studied and two of these among others (Table 2) are analysed and presented below. The selection of these two SF events was aimed at illustrating the occurrence of weak and strong SF over South Africa during strong storm periods. The statistical features of SF phenomena over the South African region has been reported by Amabayo et al. (2011). Some of the SF events observed during the high solar activity period (2001–2003) are presented in Table 2.

This table shows that most of the SF events occur during geomagnetically quiet conditions (i.e. K-index < 5). The K-index used in this study is archieved at the Hermanus Magnetic Observatory located in Hermanus (19.22°E, 34.42°S), South Africa. The K-index is the overall geomagnetic condition of the ionosphere over the past 3 h and ranges quasi-logarithmically from 0 to 9. It is directly related to the maximum amount of fluctuation (relative to a quiet day) in the geomagnetic field over a 3-h interval. In Table 2, K-index 4-3 implies that 4 corresponds to the first 3-h (say 18-21 UT) and 3 to next 3-h (21-24 UT).

2.1. March/April 2001 spread F event

SF event (in Fig. 1) is an example of weak SF occurrence during a strong geomagnetic storm activity. The SF

Table 2
Statistics of some selected days of SF occurrence.

Station	Date	Time (UT hour)	K-index	Station	Date	Time (UT hour)	K-index
MU12K	2001-03-05	03:00–03:30	4	GR13L	2002-07-08	18:00–23:30	1-3
MU12K	2001-06-04	21:30–23:30	2	GR13L	2002-07-09	00:00–03:30	2
MU12K	2001-06-05	00:00–03:00	1	GR13L	2002-07-11	00:00–04:00	0
GR13L	2001-07-17	18:00–23:30	1	GR13L	2002-08-03	00:00–03:30	4-3
MU12K	2001-09-07	18:30–19:00	0	GR13L	2002-08-03	20:00–23:30	2-3
GR13L	2001-09-09	18:30–22:00	0	GR13L	2002-08-04	00:00–01:30	4
GR13L	2001-09-15	22:30–23:30	3	GR13L	2002-08-04	20:00–23:30	2-0
GR13L	2001-09-16	00:00–02:00	2	GR13L	2002-08-05	00:00–01:30	0
GR13L	2001-11-01	22:00–23:30	2	GR13L	2002-08-27	18:30–23:00	1-4
MU12K	2002-01-01	22:00–23:30	1	GR13L	2002-08-28	00:30–02:00	3
GR13L	2002-04-14	00:00–03:30	3	GR13L	2002-09-02	20:00–23:30	0
GR13L	2002-05-14	03:00–04:30	4	GR13L	2002-09-03	00:00–03:30	0-1
GR13L	2002-05-14	18:00–21:30	5-4	GR13L	2002-09-05	02:00–03:30	1-3
GR13L	2002-05-17	01:00–02:30	1	GR13L	2002-09-06	00:00–03:30	2
GR13L	2002-07-04	22:00–23:30	2	GR13L	2003-05-30	01:30–03:00	6-4
GR13L	2002-07-05	00:00–03:30	1	GR13L	2003-09-08	00:00–02:45	0
GR13L	2002-07-06	18:00–23:30	4-3	GR13L	2003-09-19	02:00–03:45	4-3
GR13L	2002-07-07	00:00–03:30	4-0	MU12K	2003-10-29	00:30–02:00	4

occurrence observed here are within a short frequency range (2–6 MHz) compared to those observed in 2002 (Figs. 7 and 8). The interest in this particular SF event is to illustrate the occurrence of weak SF over South Africa during very strong geomagnetic storms. Fig. 1 shows that the overlapping echoes from the scattering medium causing the SF events appeared from 01:00 to 01:30 UT at a virtual height of ~300 km on 31 March 2001. The virtual height at which the diffuse echoes get reflected increased to ~450 km from 02:00 to 03:30 UT on the same day. The change in virtual height continues up to 04:30 on 02 April 2001. The variability of this height signifies the delay imposed on the signals by the spatial density variations in the scattering medium.

According to Lu (2006), co-rotating high speed solar streams, CMEs and interplanetary shocks are the most common causes of geomagnetic disturbances in the Earth's magnetosphere and ionosphere. To understand the cause and effect of irregularities causing such SF, the variability of auroral electrojet (AE) index and the disturbance storm time (Dst) index was investigated. In addition, solar wind parameters such as ion number density (Nion), solar wind speed (Vp) and IMF component Bz were also analysed for the periods of SF events (see Fig. 2). Fig. 2(a) shows northward Bz at ~01:00 UT on 31 March 2001 followed by a southward direction change of Bz component up to ~06:00 UT on 31 March 2001. The southward Bz polarity ostensibly marked the sudden storm commencement (SSC) due to the arrival of solar wind shock waves as observed by the ACE satellite (00:00–02:00 UT) on 31 March 2001. A distinct shock wave observed at ~06:00 UT on 31 March 2001 initiated the expansion phase of the strong geomagnetic storm with long lasting recovery phase. It can be seen from Fig. 2 that the southward polarities of IMF (Bz) are very well correlated with decrease and increase of Dst and AE indices respectively. The auroral activity increased (AE $\geqslant$ 500 nT) from midnight on 31 March 2001 before the storm started and decreased from around 09:00 to 11:00 UT. The onset of increased auroral activity coincides with increased solar wind plasma speed from midnight in Fig. 2(e) and this was preceded at 20:00 UT (on 31 March 2001) by an increased solar wind speed. The speed again increased up to 800 km/s at 06:00 UT on 01 April 2001 when auroral activity also increased.

Fig. 2(f) shows sharp electric field gradients between ~01:00 UT (on 31 March 2001) and ~00:00 UT (on 01 April 2001). Rapid increase in the ion number density and speed of the solar wind often leads to compression of the dayside magnetosphere. The effect of the resulting storm increases magnetic reconnection on the dayside magneto pause allowing solar wind particles to flow into the ionosphere. Reconnection is normally accompanied by a sudden release of energy stored in the oppositely directed magnetospheric magnetic fields. This leads to increased Poynting flux into the ionosphere and enhanced magnetospheric convection. Strong neutral winds are then created as a result of the corresponding Joule heating. Perturbations within thermospheric wind system may produce additional electric fields by dynamo effect (Kumar et al., 2008). Space Weather Prediction Centre (SWPC) of the United States reported a high energy solar particle event on 29 March 2001 at 16:35 UT that reached the Earth on 30 March 2001 at 06:10 UT. This was associated with the release of the halo CME at 10:26 UT on 29 March 2001 caused by a solar flare activity on this day at 10:15 UT (http://www.swpc.noaa.gov/ftpdir/warehouse/).

Several research groups have attributed mid-latitude SF with locally generated instabilities within the bottomside of the F region. The F region electric field drifts are believed to be caused by differences in the ionisation. To investigate ionospheric response towards the above storm, ionospheric data for hmF2 and h′F was extracted using SAO Explorer

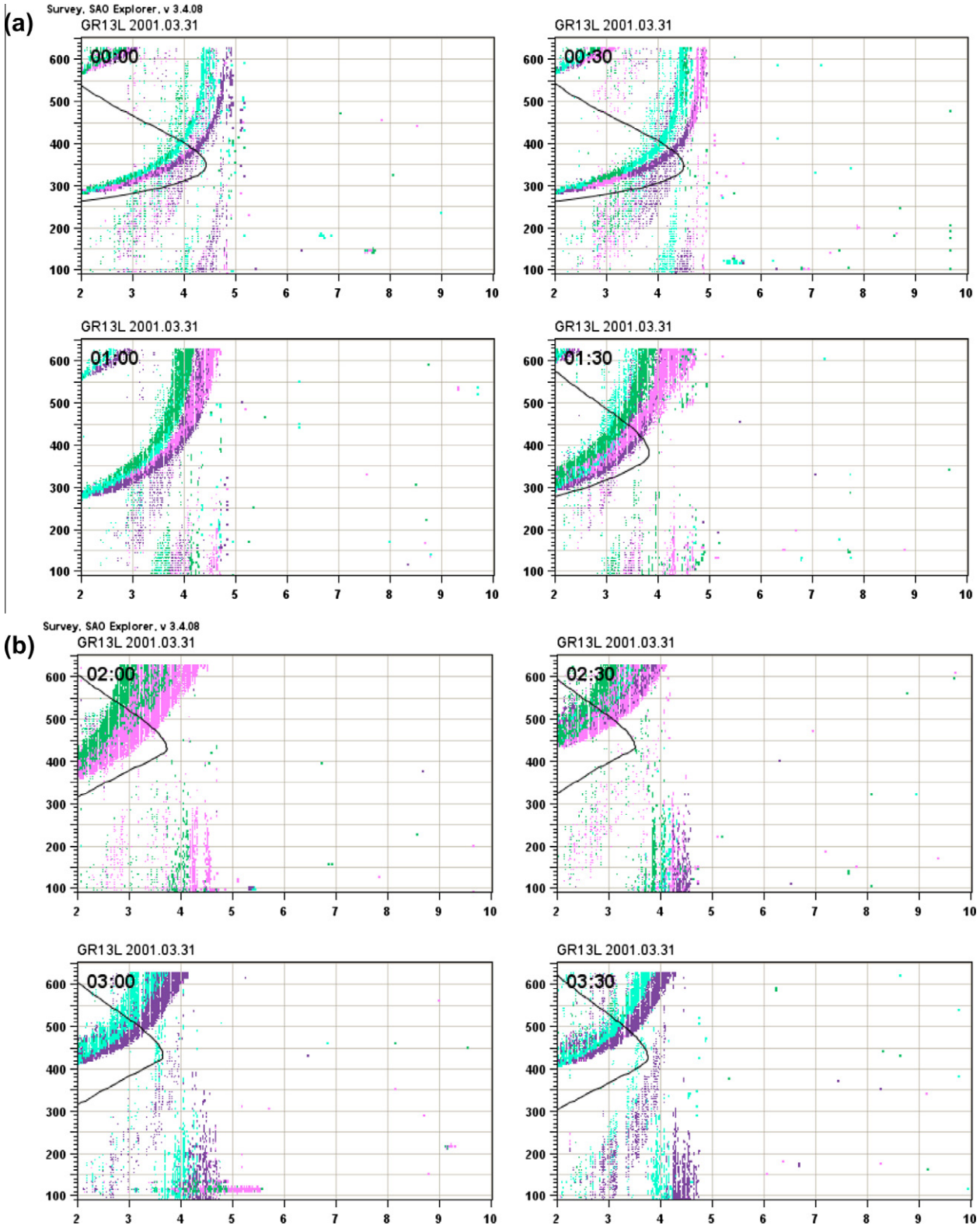

Fig. 1. Grahamstown (GR13L) ionograms showing occurrence of post-midnight occurrence of weak SF from 31 March 2001 to 02 April 2001.

software (Reinisch et al., 2005). The data during SF occurrence from Grahamstown (26.50°E, 33.32°S) was compared with that from Madimbo (30.88°E, 22.38°S) station (Fig. 3). This helps to understand and trace the mechanisms responsible for the SF occurrence over this region. The values of hmF2 and h′F observed at Grahamstown are slightly higher compared to those observed at Madimbo, except around midday on 02 April 2001 when

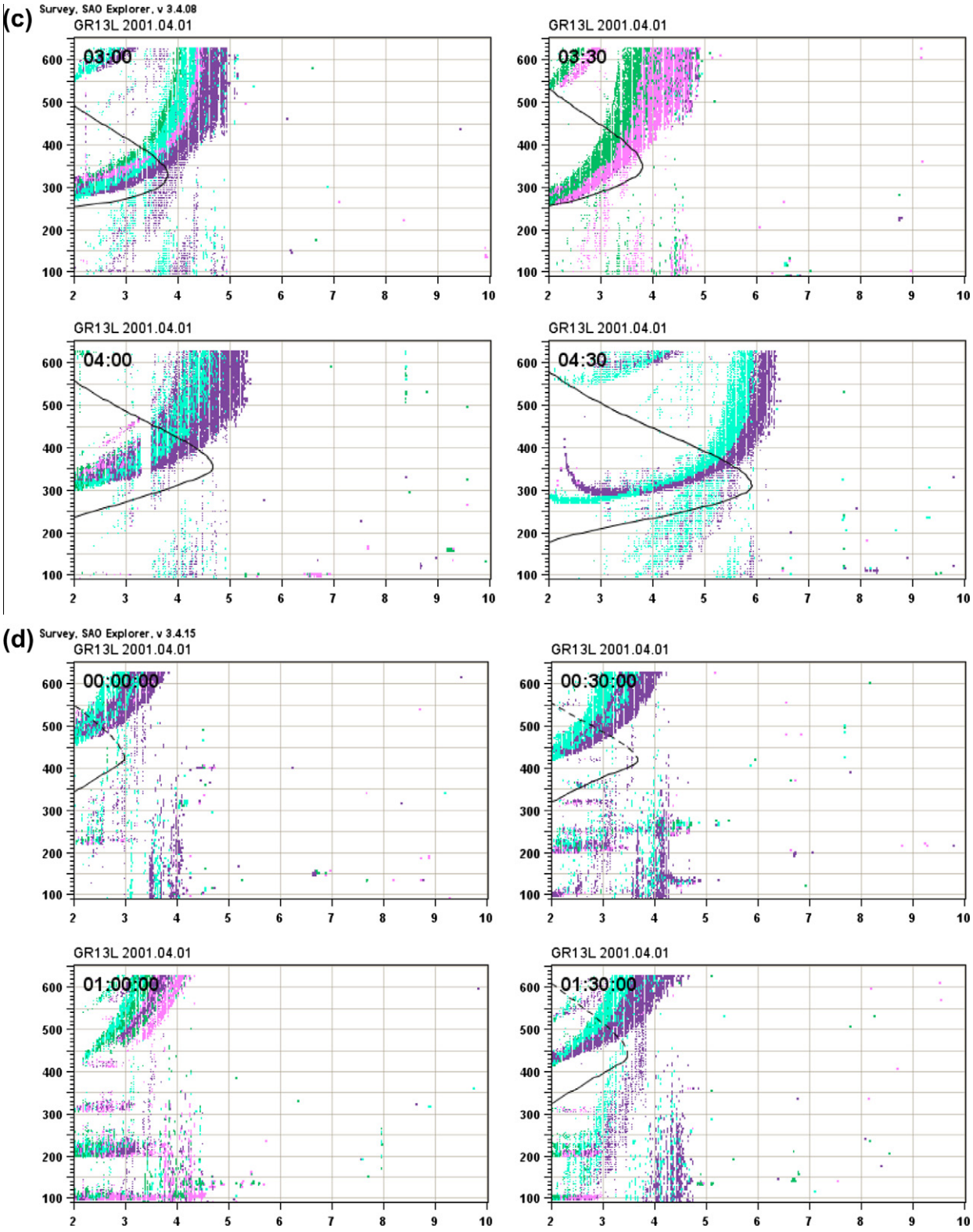

Fig. 1. (*continued*)

h′F at Madimbo became higher. The highest value of h′F ($\geqslant$400 km) between 18:00 and midnight on 01 April 2001 (Fig. 3(b)) is consistent with the main phase of the storm in Fig. 2. The value of h′F decreased below 400 km from midnight to 03:00 UT during the recovery phase of the storm on 01 April 2001 during which SF was observed. The uplift and decrease of h′F is attributed to positive and negative storm effects respectively. Depletion of the

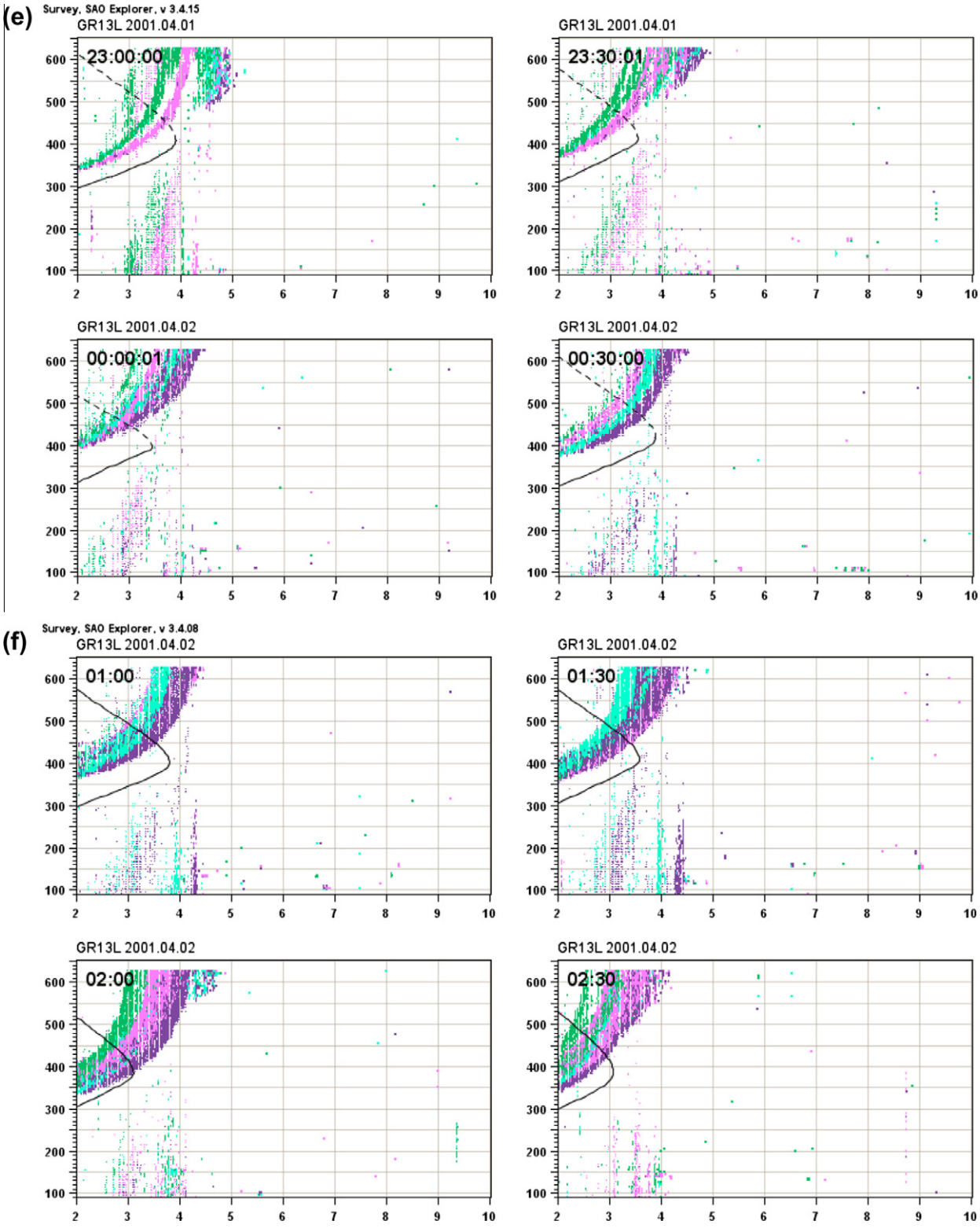

Fig. 1. (*continued*)

ionospheric plasma due to storm induced effects often causes thinning of the F layer, particularly at night. At night recombination takes place and this leads to decrease in electron/ion density and hence a decrease in TEC is expected. During increased ionospheric activity periods, the height of the F2 layer is unstable and thus shows high variability (evident between ~00:00 and 06:00 UT and 18:00 and 06:00 UT on 31 March 2001). The ionosphere being embedded in the thermosphere is subject to the influence of thermospheric winds. These neutral winds blow

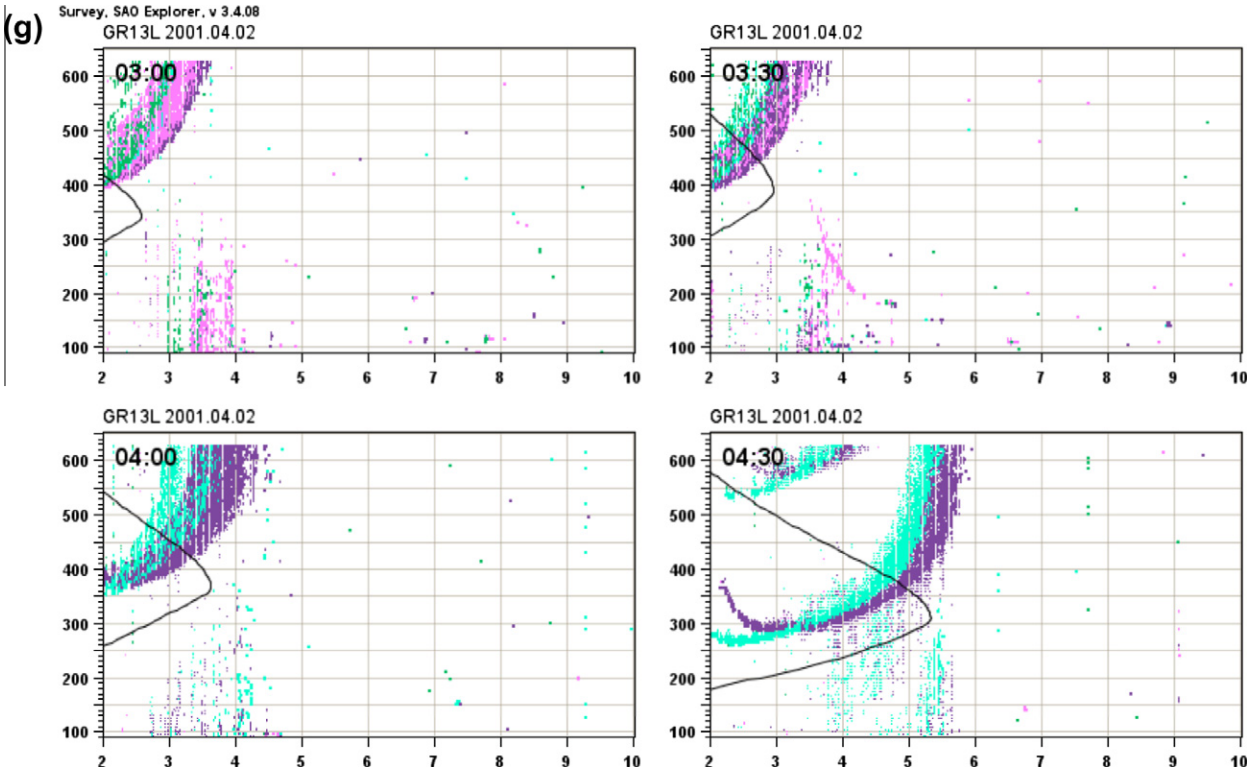

Fig. 1. (*continued*)

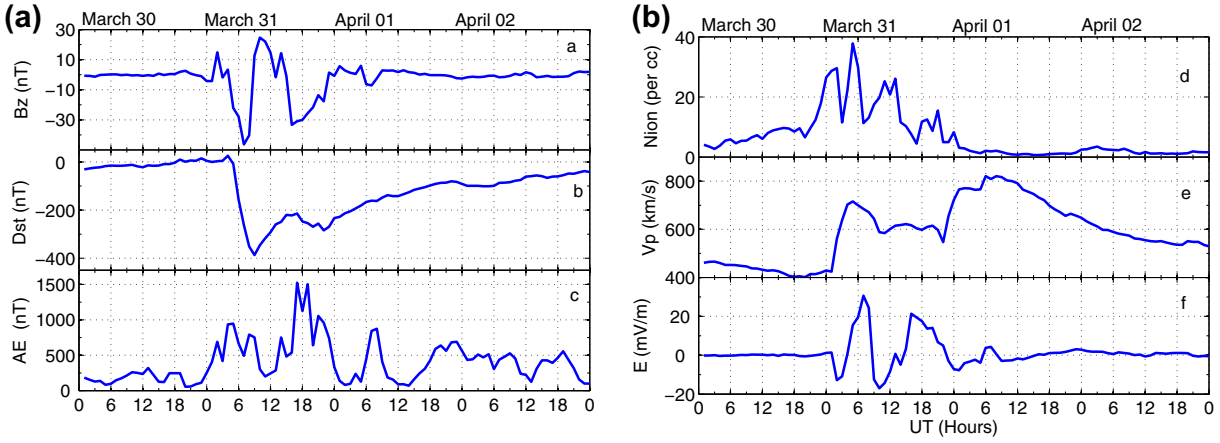

Fig. 2. (a) IMF (Bz) with several southward turnings during the peak storm phases. Variability of hourly (b) Dst and (c) AE indices. (d) Ion number density (Nion) with sharp gradients. (e) Solar wind plasma flow speed (Vp) during the disturbed days. (f) Variability of convection electric field (E). (Data source: ACE website http://cdaweb.gsfc.nasa.gov/cdaweb/sp_phys/.)

and drag the ionosphere along, and hence influences the dynamics of the ionosphere at such locations (Davies, 1990). Changes in the flow of the winds at a given time and location causes diurnal variations of ionospheric parameters such as hmF2, h′F and TEC. During severe storms, increased influx of charged and energetic particles into the ionosphere can enhance the amplitude of ionospheric irregularities. The time derivative of h′F (Vd) shows a high variability in the ionospheric plasma from 00:00 to 06:00 UT during the strong storm on 31 March 2001 (Fig. 3(c)). However, the drift velocity (Vd) reflected in Fig. 3(c) is slow, except on 31 March 2001 between 00:00 and 06:00 UT. The high variablity of Vd within this interval coincides with the SSC of the strong storm. This may be attributed to the impulse caused by arrival of the shock waves on the magnetosphere within this interval.

An attempt was made to investigate the derived *VTEC* data from available GPS receiver stations. This was aimed at reconciling the GPS measurements and the F region ionospheric parameters obtained from ionosonde data.

The *VTEC* observed from all the four stations shows a decrease in TEC from ~8:00 to 10:00 UT and 11:00 to

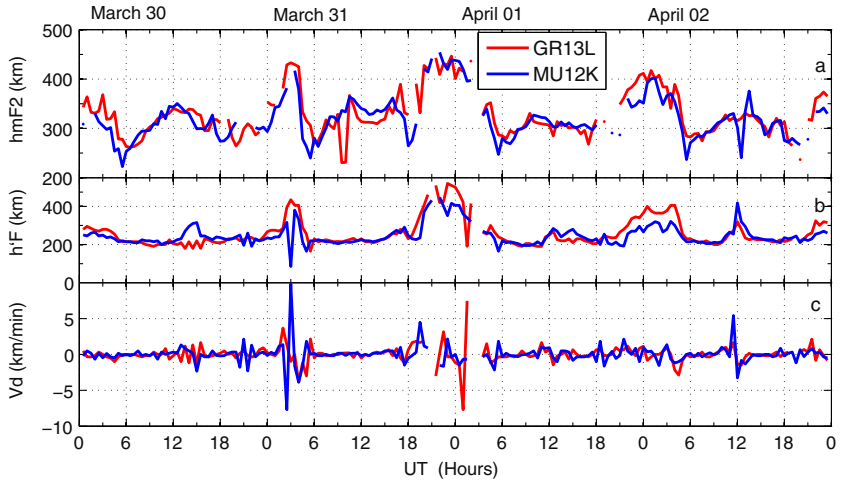

Fig. 3. Variability of (a) maximum height of the F2 layer (hmF2) and (c) F2 layer bottom height (h′F) from 30 March to 02 April 2001. (c) Time derivative (Vd) of F2 layer bottom height (h′F).

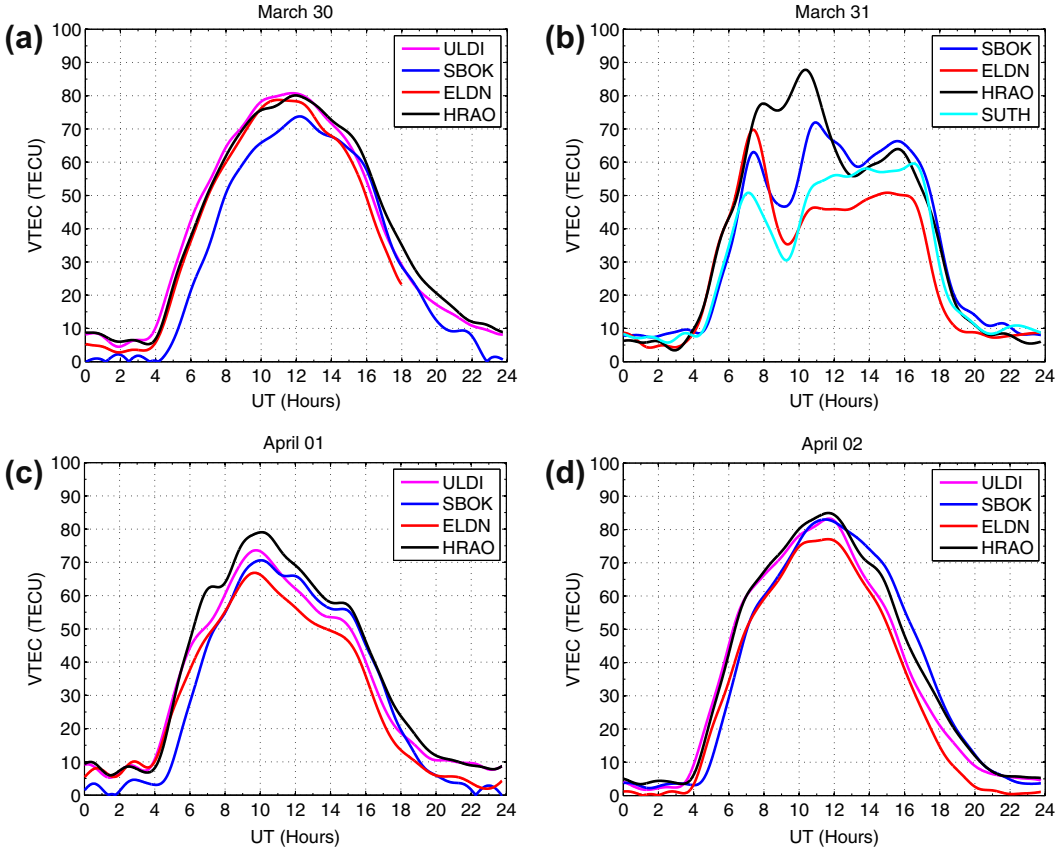

Fig. 4. Variability of the *VTEC* during quiet and disturbed days for different four stations.

16:00 UT on 31 March 2001 (Fig. 4(b)). The decrease in the TEC at these intervals coincides with the arrival of shock waves as observed by ACE satellite (Fig. 2). The normal diurnal pattern of TEC exhibits a steady increase from about sunrise to an afternoon maximum when the Sun is overhead and then falls to a minimum just before sunset as in Fig. 4(a), (c) and (d). The decrease in TEC (Fig. 4(b)) is attributed to storm induced ionospheric plasma density perturbations occurring during the onset of decreased solar wind speed in Fig. 2(e).

The *VTEC* at the IPPs was also plotted to examine the locations of TEC gradients which may have led to TEC perturbations. The diurnal and latitudinal pattern of *VTEC* was also examined by looking at different longitudinal sectors. This was done by computing TEC using data from all the receivers combined with one receiver chosen

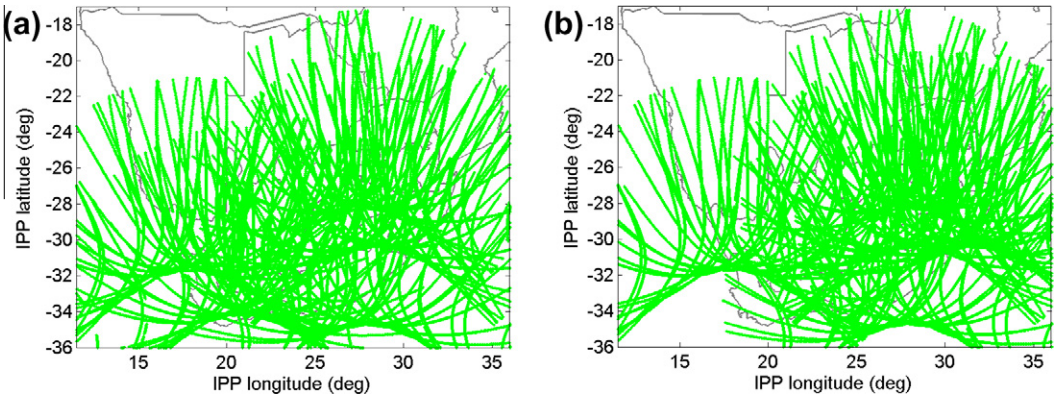

Fig. 5. Coverage of the IPPs observed from the four receivers on (a) 31 March 2001 and (b) 01 April 2001.

as the interpolation point. The *VTEC* along particular IPP longitudes was plotted. The IPPs of the satellites visible at each receiver station are shown in Fig. 5(a) and (b). This helps to explain the observed diurnal and latitudinal distribution of TEC over South Africa during the strong storm event. The choice of the latitude range entirely depends on the IPP latitude coverage for the day. Fig. 5(a) and (b) shows that the IPPs based on the four receivers in Fig. 4(b) and (c) displays a fair coverage of the South African region. The ASHA algorithm interpolation yields good TEC results in regions well covered by the IPPs. The ASHA algorithm extrapolation outside the IPP coverage gives rise to wrong TEC (i.e. high ±TEC). Therefore, the diurnal and latitudinal TEC variability in Fig. 6 were obtained by using the IPP latitude range of −34° to −23°. The TEC variation along particular IPP longitudes was then investigated as below. It should be noted that the fewer the receiver stations used, the poor the IPP coverage which in turn affects the TEC values.

The diurnal trend in Fig. 6 shows that the TEC is low during the nighttime (00:00 to 05:00 UT and 18:00 to 24:00 UT) and high during the day. The peak of the TEC can be observed between 07:00 and 12:00 UT. The TEC values during these intervals are higher at low mid-latitudes (∼23.5–29.5°S) and lower at mid-latitudes (∼30–34°S). The diurnal and latitudinal pattern of TEC observed at the four selected meridian longitudes (17°E, 23°E, 27°E and 33°E) are identical. This implies that the TEC over South Africa on this day was independent of longitude. The occurrence of TEC decrease (or depletion) due to the satellite signals encountering ionospheric irregularities can be observed between ∼06:00 and 11:00 UT. The TEC decrease within this time interval (also observable in Fig. 4(b)) occurs in the IPP latitude range TEC values during these intervals are higher at low mid-latitudes 34° to TEC values during these intervals are higher at low mid-latitudes31° (mid-latitude zone) for all meridian longitudes considered. The TEC values on the right panel of Fig. 6 occur during the recovery of the ionosphere from main phase of the strong storm.

2.2. 07 September 2002 spread F event

This event is another example of SF occurrence during high solar activity observed at three ionosonde stations during spring in 2002. Although only Madimbo and Louisvale ionograms have been shown, there was also SF observed from Grahamstown starting from 00:00 to 03:30 UT on 07 September 2002. The intensity of the SF observed from Grahamstown (not shown) was lower than the intensity observed from Madimbo and Louisvale (21.24°E, 28.51°S) as shown in Figs. 7 and 8. The frequency at which reflections occur can be observed to increase from 8 MHz up to 11 MHz. The irregular structure suddenly appeared at 18:30 UT at Madimbo and 19:00 UT (30 min later) at Louisvale. *These perturbations are most likely associated with the occurrence of prompt penetration electric fields, produced during the southward turning of the IMF component (Bz). This prompt penetration phenomenon can cause ionospheric uplift due to enhanced $E \times B$ drift and increased TEC. These F region electric field drifts are believed to be a consequence of the differences in the ionisation.* Geomagnetic and solar wind data obtained from ACE satellite was examined as shown in Fig. 9.

During a magnetic storm the plasmasphere opens up due to magnetic reconnection and loses its plasma to the magnetotail, consequently depleting plasma in the ionosphere in the process (Fuller-Rowell et al., 1990, 1994). Hence, during and after a geomagnetic storm, both positive and negative ionospheric changes in ionospheric density are observed, mostly noticeable in the F2 layer. According to Prölss (1993), these positive and negative ionospheric storm effects are believed to have strong local time dependence. Negative storm effects are the dominant characteristic in the ionospheric response to geomagnetic activity enhancements (Belehaki and Tsagouri, 2001). Generally it has been accepted that negative storm effects are attributed to neutral composition changes during which increases in molecular ion species tend to hasten the ion recombination which in turn may slow the rate of increase or cause a decrease in plasma density (Fuller-Rowell et al., 1994).

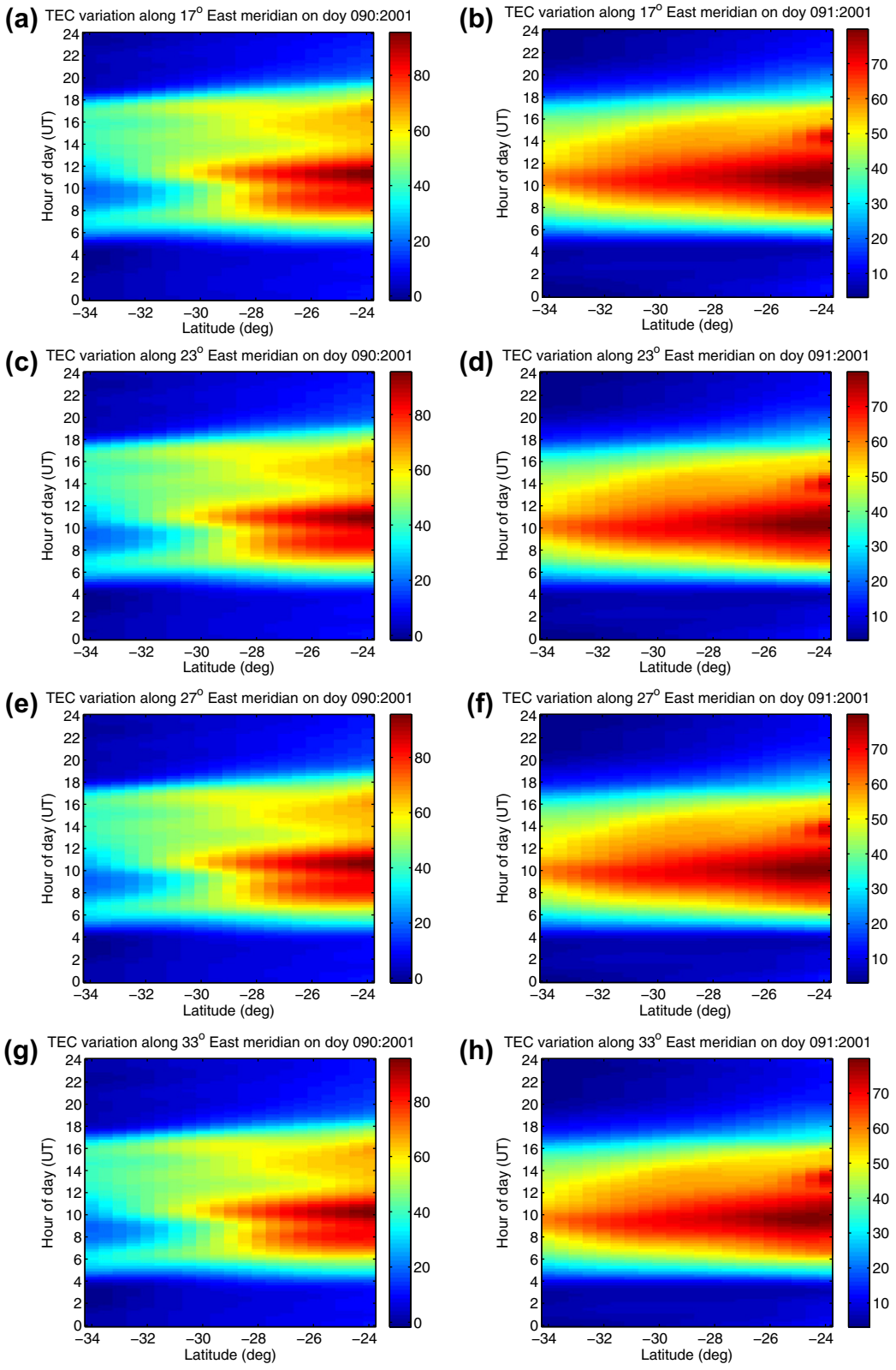

Fig. 6. The variation of *VTEC* with time of the day and IPP latitude on 31 March 2001 (left panel) and 01 April 2001 (right panel).

The Space Weather Prediction Centre (SWPC) reports show that high energy solar particle (>10 MeV) event started on 07 September 2002 at 04:00 UT (http://www.swpc.noaa.gov/ftpdir/ or http://cdaw.gsfc.nasa.gov/CME_list/). This event was attributed to a halo CME released on 05 September 2002 at 16:50 UT (associated with a C5 flare on 05 September 2002) which affected the Earth's environment. The occurrence of shock waves

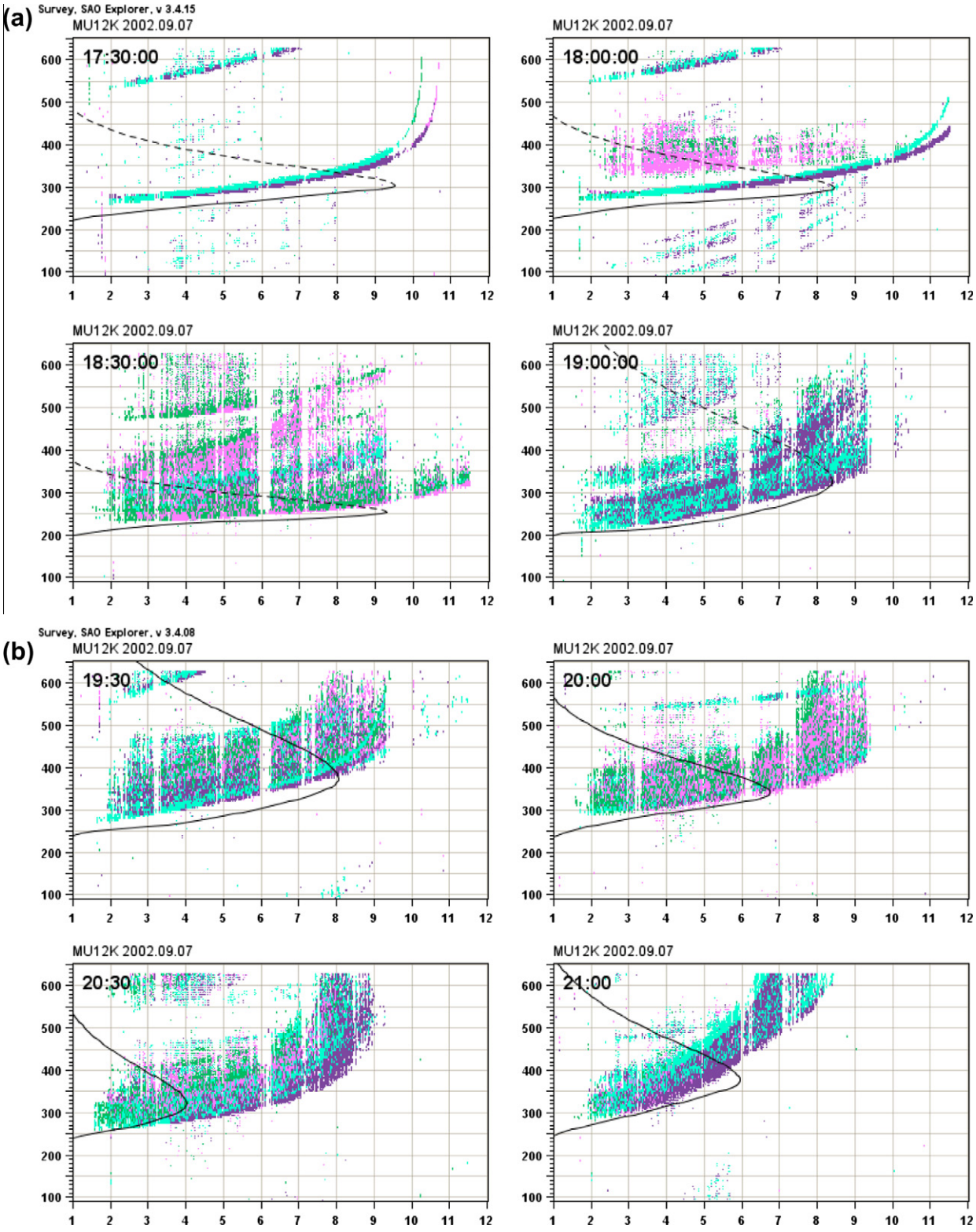

Fig. 7. Ionograms showing intense SF occurrence between 18:00 and 23:00 UT as observed from Madimbo on 07 September 2002.

between ~15:00 UT (on 07 September 2002) and 06:00 UT (on 08 September 2002) is initiated by the ring current direction change, thus the southward turnings of the Bz indicate a reconnection process, during which the magnetic field lines of the Earth open up and thus allowing solar wind particles to penetrate the ionosphere. The induced strong storm with minimum Dst of ~ -200 nT is sufficient to influence changes in the ionosphere. The increase in ion number density from 12:00 UT (on 07 September 2002) to ~08:00 UT (on 08 September 2002) which shoots up at

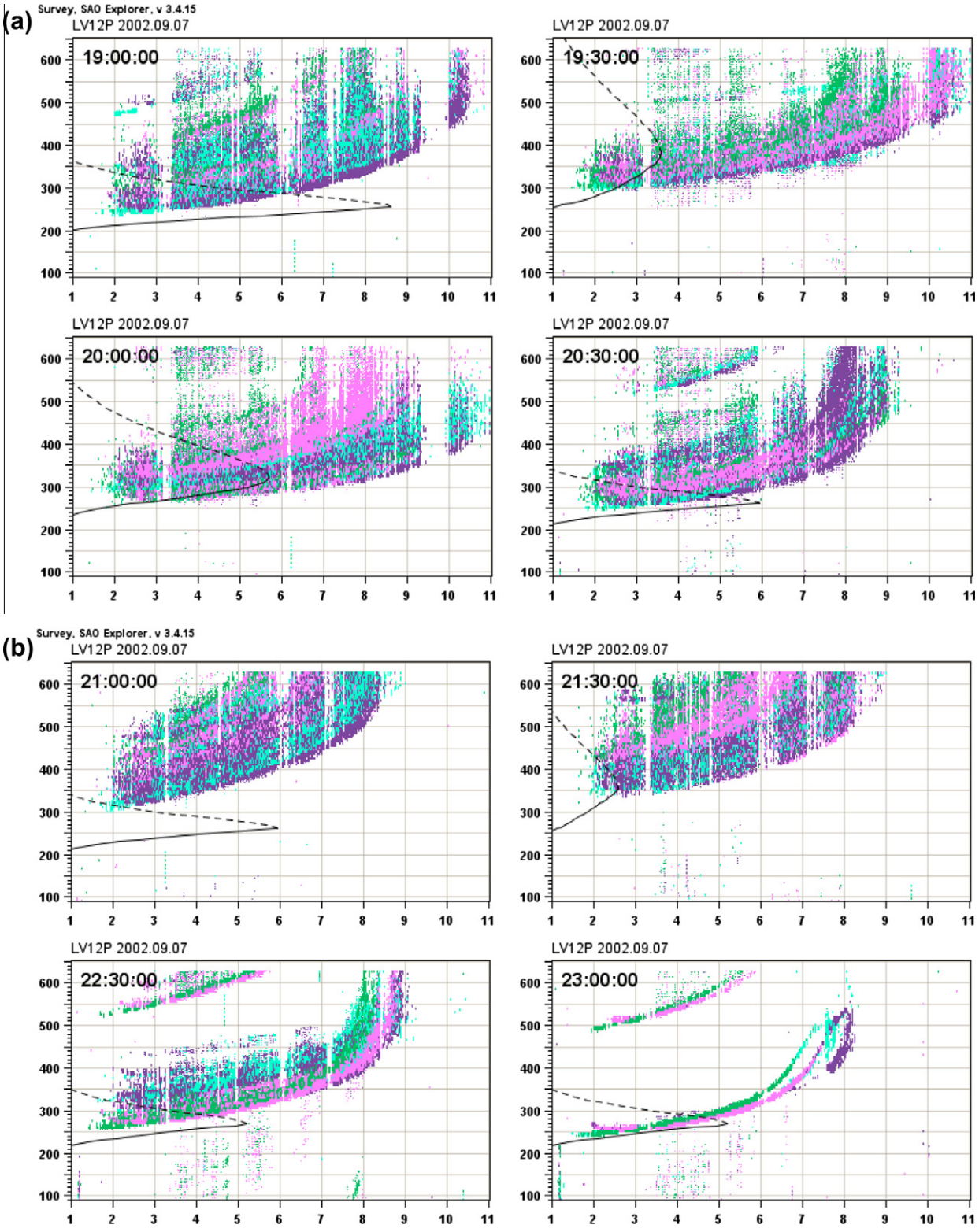

Fig. 8. Ionograms showing intense SF between 18:00 and 23:00 UT as observed from Louisvale on 07 September 2002.

~06:00 UT on 08 September 2002 are evidences of changes induced in the ionosphere due to the storm. The increased ionisation associated with positive storm effects are attributed to the neutral wind effect starting at auroral latitudes where perturbed interactions between the solar wind and the magnetosphere yield increased energetic particle precipitation, convection electric fields and associated Joule heating. The induced electric field due to convection was highly variable during the period above (12:00 UT to ~08:00 UT) and there was a sudden increase of plasma speed. The Joule

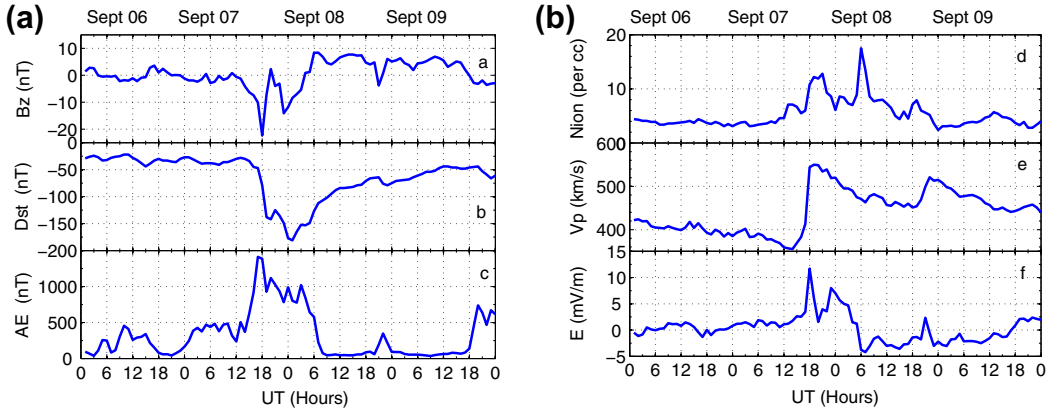

Fig. 9. (a) Variability of IMF (Bz) field with southward minimum value of −22 nT at 18:00 UT from 06 to 09 September 2002. The variability of hourly (b) Dst index, (c) AE index, (d) ion number density, (e) plasma flow speed and (f) electric field for the same period.

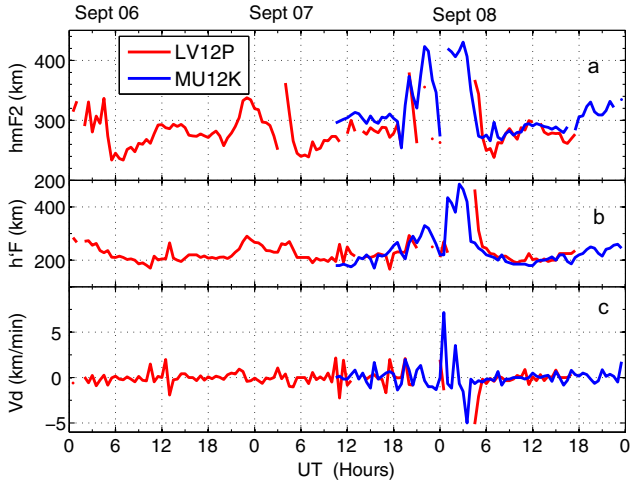

Fig. 10. Variability of (a) hmF2 and (b) h′F as observed from Madimbo and Louisvale stations from 06 to 08 September 2002. (c) The time derivative of the F2 layer bottom height for the same period.

heating raises the thermosphere temperature at auroral latitudes, resulting in enhanced equatorward winds and TIDs (Jodogne and Stankov, 2002).

A further investigation of the effect of the irregularities induced by the storm on the ionosphere was conducted using ionosonde data. The depression and uplifting of the ionospheric parameters during perturbed conditions was studied by analysing the hmF2 and h′F. These two parameters are chosen because they are not affected much by the occurrence of SF and hence their variability is paramount in identifying perturbations in the F layer. The data for these parameters was compared for two stations (Fig. 10). The ionospheric storm effect in Fig. 10 is explained in terms of positive and negative storm effects. The values of hmF2 and h′F shoot up between ~18:00 UT (on 07 September 2002) and 06:00 UT (on 08 September 2002), and remained low for the other periods of the days. Higher values of h′F with respect to hmF2 during this period may be attributed to enhancement of the ionospheric plasma due to the strong positive storm effect. The effect of the nighttime enhancement caused by an irregularity is higher at Louisvale compared to Madimbo. The high rate of plasma density depletion could be the cause of lower values of hmF2 and h′F from Louisvale than Madimbo.

The effect of the storm on GPS TEC was also investigated using available data from the selected dual frequency GPS receivers. The result of derived *VTEC* and the perturbations observed from the stations with reliable data are shown in Fig. 11(a) and (b) respectively.

The *VTEC* is observed to depart by ~5 and ~20 TECU from the mean value at PRET/HRAO and SUTH/ SBOK on 08 September 2002 respectively. The *VTEC* and mean *VTEC* are approximately the same on 07 and 09 September 2002 (Fig. 11(a)). There is a sudden TEC increase just after 18:00 UT observed at HRAO and SBOK on 07 September 2002. This nighttime TEC enhancement may be attributed to a combination of processes (e.g. neutral wind composition changes and TIDs) as a result of storm induced perturbations. Under ordinary conditions, the diurnal pattern of TEC (i.e. a normal curve) is that TEC is low during the night and high during the day. The reason for this is that during daytime, EUV (extra ultraviolet) from the Sun ionises the atmosphere of the Earth thus increasing the TEC, while the nighttime values of TEC are reduced due to chemical recombination (Davies, 1980). Rapid TEC fluctuations may occur instead of smooth variations during ionospheric disturbance due to magnetic storms or density perturbations. The perturbations induced in the TEC was examined for the four stations as discussed below.

The perturbed *VTEC* observed in Fig. 11(b) reflect turbulent ionosphere under the influence of strong geomagnetic disturbance. A variable *VTEC* perturbation can be observed in Fig. 11(b) from 18:00 UT (on 07 September 2002) to 00:00 UT (09 September 2002). Sudden increase in auroral and storm activity was observed previously observed at 18:00 UT (see Fig. 8) which in turn led to increased ion number density and prompt penetration of electric fields. The sudden increase in *VTEC* at 18:00 UT (on 07 September 2002) may be attributed to the injection

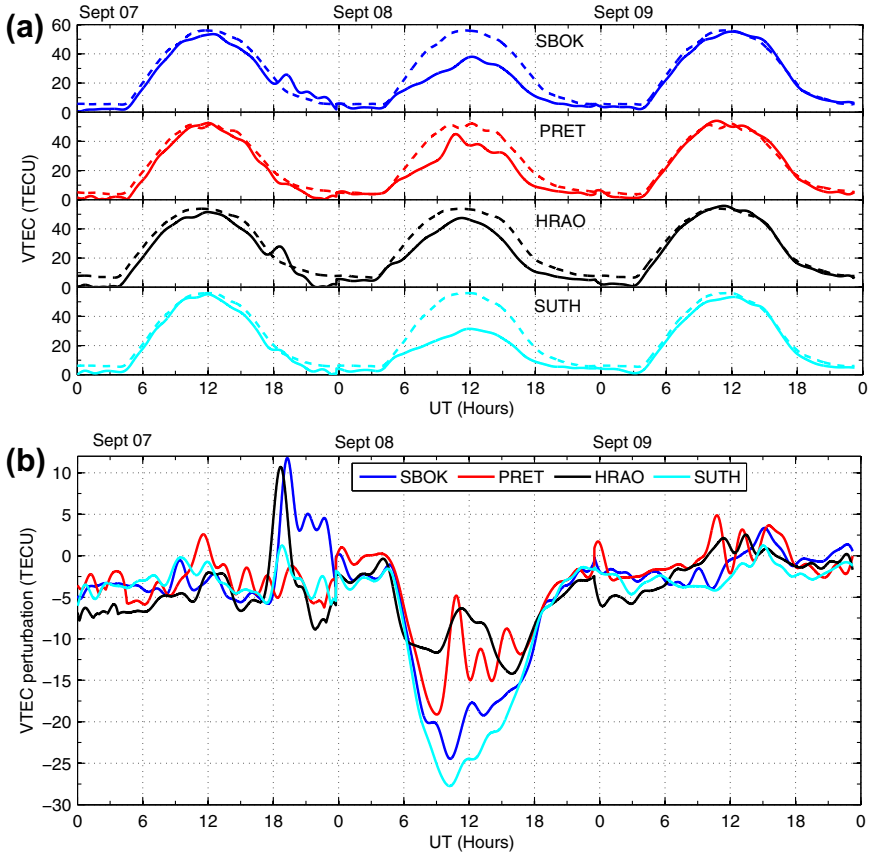

Fig. 11. (a) Variability of the disturbed *VTEC* (solid lines) and the mean *VTEC* (dashed lines) for the four stations. (b) The derived TEC perturbation for GPS stations with data availability during the geomagnetically disturbed period.

of energetic particles in to the ionosphere system during a reconnection process. The perturbed *VTEC* in Fig. 11(b) shows higher values at SBOK and HRAO than PRET and SUTH (between 17:00 and 00:00 UT on 07 September 2002), where negative storm effects were observed as depicted by the depression of the TEC.

The phenomena of TEC decrease and increase was further investigated by analysing TEC along the ray path between individual satellites and the receiver stations. The results are an indication of the satellite paths that encountered the ionospheric irregularities responsible for the TEC perturbations observed at the receiver stations (Fig. 12). It should be noted that TEC observations when the satellites are below 20° elevation are considered as multipath effect in this study.

The TEC observed along the ray path between pseudo-random number (PRN) 15 and the receiver at Pretoria shows a decrease (>8 TECU) between 19:00 and 21:00 UT. This was followed by a TEC increase and a decrease from 21:00 to 23:00 UT. A similar TEC pattern was observed along the ray path between PRN 17 and the receiver at Pretoria. It can be observed that PRN 17 encountered small scale irregularities between 21:00 and 22:00 UT. The decrease and increase in the TEC observed along the ray path between PRN 15 and Springbok lags behind the observation made at Pretoria by ~2 h. Series of the small scale irregularities were encountered along this path between ~20:30 and 23:00 UT. The nature of the TEC along the ray path between PRN 17 and Springbok is similar to that of PRN 15 and also lags behind by about the same duration of time (2 h). The TEC along the ray path between PRNs 15 and 17, and the receivers at Pretoria and Springbok shows opposite signs within a given interval of time (i.e. TEC increase and decrease, and vice versa). This can be observed for example between 18:00 and 19:00 UT when TEC increase and decrease were observed between these two receivers and PRN 17. The trend of TEC observed along the ray paths between satellites 18 and 23, and Springbok also reveals presence of small scale irregularities at the intervals 19:00–23:00 UT and 19:00–20:00 UT. TEC enhancement was observed along the ray paths between PRNs 15 and 17 and Sutherland between 21:00 and 22:00 UT. The fact that these observations were made above 20° implies presence of density irregularities that caused the observed TEC perturbations. The local time difference between these receivers was considered and time shifts were observed between HartRAO and Pretoria which have ~0.6° longitude difference (Table 1). The dynamical causes of negative TEC phase effects are quite distinct from those due to enhanced chemical losses. Composition changes resulting from storm-induced modifications to thermospheric circulation are known to be the dominant driving mechanisms

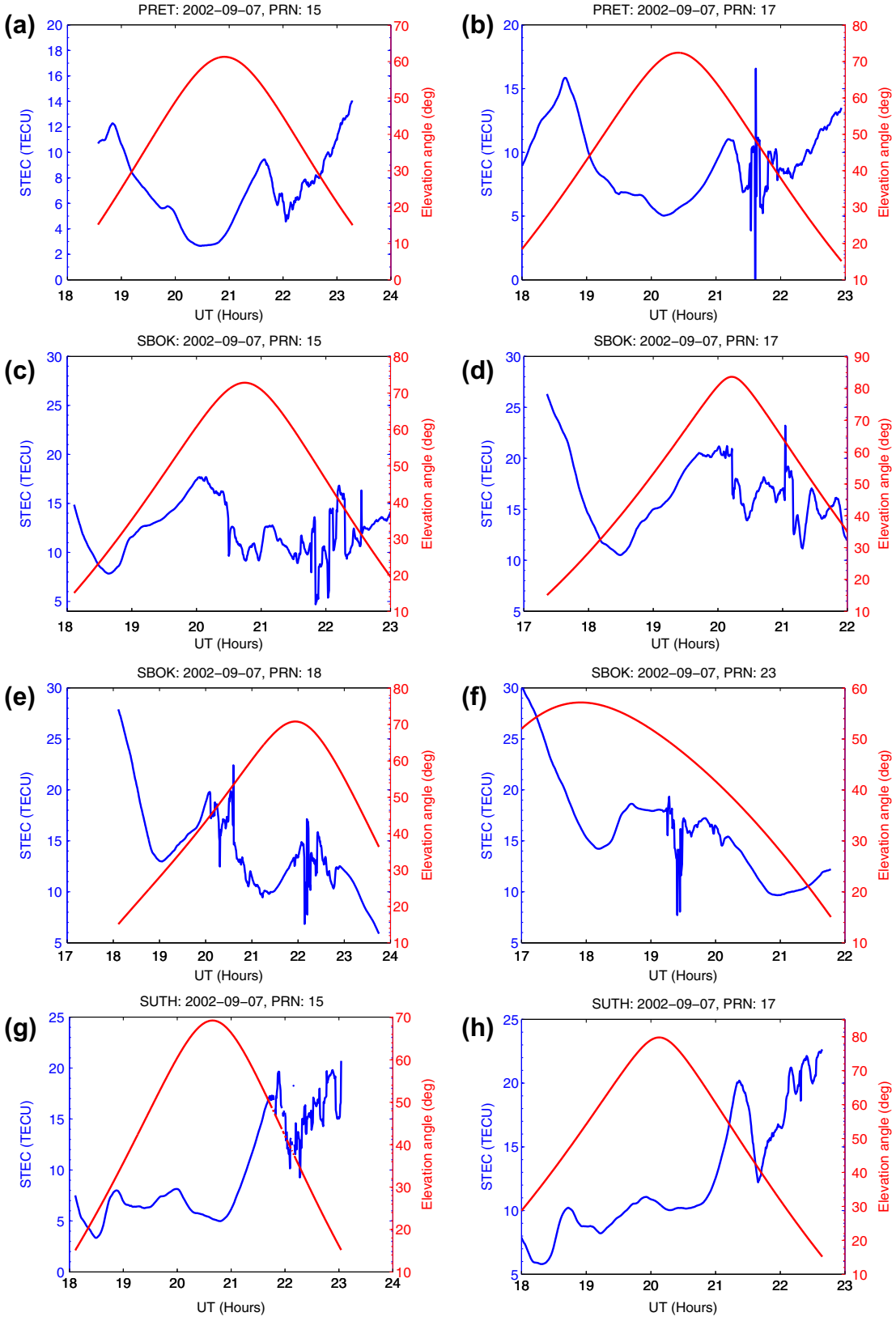

Fig. 12. Elevation angle and *STEC* as observed at the four GPS receiver stations as a function universal time (UT).

of the daytime negative phase at mid-latitudes. Time shift of about 13 min were obtained after removing local time effects between HartRAO and Pretoria. This time shift is attributed to the effect of enhanced equatorward winds which launch TIDs during their propagation (Jodogne and Stankov, 2002).

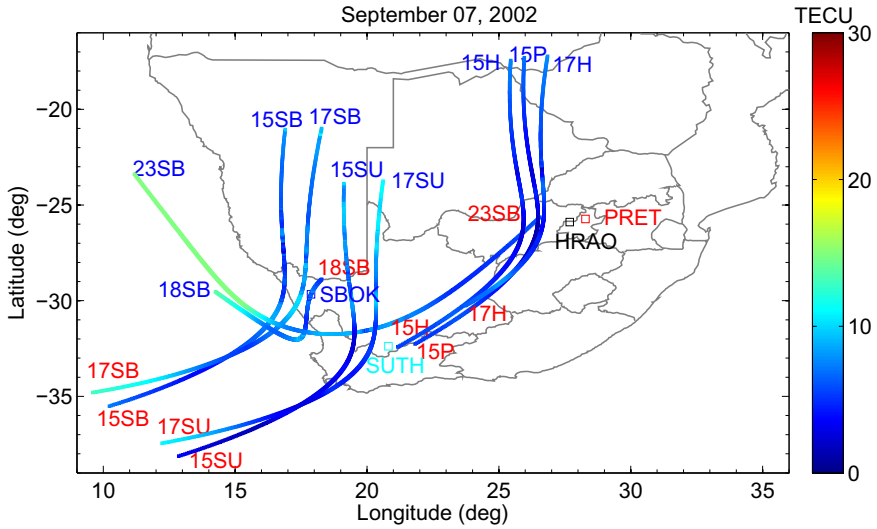

Fig. 13. Map of South Africa showing the *VTEC* at IPP for selected satellites observed at Springbok, East London, HartRAO and Sutherland GPS receiver stations.

After establishing the ray paths encountering irregularities, the next interest in this study was to trace the IPP locations of the irregularities. The *VTEC* observed by each satellite was mapped on the IPPs (arcs) of the satellites and the results are presented in Fig. 13. The observations in Fig. 12 shows that significant TEC gradients were observed along the ray paths to the satellites (15, 17, 18 and 23) as viewed from the four receiver stations. It should be noted that the labels in red and blue represent the start and end of the IPP arcs respectively. Some arbitrary letters have been added to the PRNs to indicate the receiver station from which each satellite was observed. The labels SB (e.g. 17SB), SU (e.g. 17SU), H (e.g. 17H) and P (e.g. 17P) refer to PRN 17 as observed from Springbok, Sutherland, HartRAO and Pretoria respectively. The decrease and increase in the TEC as a result of the irregularities encountered by the satellites are observable in the IPP positions between 16° and 25° longitude and −34° and −28° latitude.

2.3. Conclusions

Negative storm effects were observed on the ionosphere over the mid-latitude South African region during the strong geomagnetic storm from 31 March to 02 April 2001. The storm induced perturbations in the ionospheric electron concentration were examined on the ionosonde and GPS data. Increase in the TEC perturbation of magnitude $\geqslant$15 TECU were observed between 17:00 and 21:00 UT (at Springbok and HartRAO) during the expansion phase of the storm on 07 September 2002. A trough in the TEC perturbation was observed during the substorm and recovery phases of the storm on 08 September 2002 between 06:00 and 12:00 UT. The TEC perturbation in Fig. 11 revealed storm-induced TIDs as the source of the irregularities observed over South Africa during the period examined. The question of the size of the irregularity structures responsible for these perturbations remained unsolved in this study. Another signature of the storm-induced irregularity over the South African region is the observed SF. The differences in the SF phenomenon observed at the three ionosonde stations on 07 September 2002 demonstrates existence of varying irregularity sizes. Therefore, this study has shown that the mid-latitude ionosphere was greatly perturbed during the two strong storms.

Acknowledgements

The authors acknowledge the management of Lowell DIDBase, Coordinated Data Analysis Web (CDAWeb) and International GPS Service (IGS) and National Geospatial Information (NGI) for the ionosonde data, Geomagnetic and solar wind data, and dual frequency GPS data respectively.

References

Amabayo, E., McKinnell, L.A., Cilliers, P. Statistical characterisation of spread F over South Africa. Adv. Space Res. 48, 2043–2052, 2011.

Belehaki, A., Tsagouri, I. Study of the thermospheric-ionospheric response to intense geomagnetic storms at middle latitudes. Phys. Chem. Earth 26, 353–357, 2001.

Blanc, M., Richmond, A. The ionospheric disturbance dynamo. J. Geophys. Res. 85, 1669–1686, 1980.

Dashora, N., Sharma, S., Dabas, R.S., Alex, S., Pandey, R. Large enhancements in low latitude total electron content during 15 May 2005 geomagnetic storm in Indian zone. Ann. Geophys. 27, 1803–1820, 2005.

Davies, K. Recent progress in satellite radio beacon studies with particular emphasis on the ATS-6 radio beacon experiment. Space Sci. Rev. 25, 357–430, 1980.

Davies, K. Ionospheric radio. Peter Peregrinus, London, 1990.

Essex, E.A., Mendillo, M., Schoedel, J.P., Klobuchar, J.A., daRosa, A.V., Yeh, K.C., Fritz, R.B., Hibberd, F.H., Kersley, L., Koster, J.R. A global response of the total electron content of the ionosphere to the magnetic storm of 17 and 18 June 1972. J. Atmos. Solar-Terr. Phys. 43, 293–306, 1972.

Fejer, B.G. Low-latitude ionospheric disturbance electric field effects during the recovery phase of the 19-21 October 1998 magnetic storm. J. Geophys. Res. 108, http://dx.doi.org/10.1029/2003JA010190, 1998.

Fejer, B.G., Scherliess, L. Mid- and low-latitude prompt-penetration ionospheric zonal plasma drifts. Geophys. Res. Lett. 25, 3071–3074, 1998.

Fuller-Rowell, T.J., Rees, D. A three-dimensional time-dependent simulation of the global dynamical response of the thermosphere to a geomagnetic substorm. J. Atmos Solar-Terr. Phys. 43, 701–721, 1981.

Fuller-Rowell, T.J., Rees, D., Tinsley, B.A., Rishbeth, H., Rodger, A.S., Quegan, S. Modelling the response of the thermosphere and ionosphere to geomagnetic storms: Effects of a mid-latitude heat source. Adv. Space Res. 10, 215–223, 1990.

Fuller-Rowell, T.J., Codrescu, M.V., Moffett, R.J., Quegan, S. Response of the thermosphere and ionosphere to geomagnetic storms. J. Geophys. Res. 99, 3893–3914, 1994.

Hoffmann-Wellenhof, B., Lichtenegger, H., Collins, J. Global Positioning System Theory and Practice. Springer-Verlag, Wien New York, 1992.

Jodogne, J.C., Stankov, S.M. Ionosphere-plasmasphere response to geomagnetic storms studied with RMI-Dourbes comprehensive database. Ann. Geophys., 2002.

Kintner, P.M., Coster, A., Fuller-Rowell, T., Mannucci, A.J. Overview of mid-latitude ionospheric storms. EOS Trans. AGU 88, 358–359, 2007.

Kumar, S., Singh, A.K. The effect of geomagnetic storm on GPS derived Total Electron Content (TEC) at Varanasi, India. In: 23rd National Symposium on Plasma Science and Technology (PLASMA-2008), vol. 208. J. Phys. conference series, 2010.

Kumar, V.V., Parkinson, M.L., Dyson, P.L., Polglase, R. Solar and geomagnetic activity effects on mid-latitude F-region electric fields. Ann. Geophys. 26, 2911–2921, 2008.

Lu, G.. Recurrent Magnetic Storms: Corotating Solar Wind Streams, second edition. Geophysical Monograph Series, vol. 167, 2006.

Opperman, B.D.L., Cilliers, P.J., McKinnell, L.A., Haggard, R. Development of a regional GPS-based ionospheric TEC model for South Africa. Adv. Space Res. 39, 808–815, 2007.

Pi, X., Mendillo, M., Fox, M.W. Diurnal double maxima patterns in the F region ionosphere: substorm-related aspects. J. Geophys. Res. 98, 677–691, 1993.

Prölss, G.W. On explaining the local time variation of ionospheric storm effects. Ann. Geophys. 11, 1–9, 1993.

Prölss, G.W., Jung, M.J. Travelling atmospheric disturbances as a possible explanation for daytime positive storm effects of moderate duration at middle latitudes. J. Atmos. Solar-Terr. Phys. 40, 1351–1354, 1978.

Prölss, G.W., Brace, L.H., Mayr, H.G., Carignan, G.R., Killeen, T.L., Klobuchar, J.A. Ionospheric storm effects at subauroral latitudes: a case study. J. Geophys. Res. 96, 1275–1288, 1991.

Reinisch, B.W., Huang, X., Galkin, I.A., Paznukhov, V., Kozlov, A. Recent advances in real-time analysis of ionograms and ionosonde drift measurements with digisondes. J. Atmos. So-Terr. Phys. 67, 1054–1062, 2005.

Wanninger, L. Ionospheric monitoring using IGS data. In: Proceedings of the 1993 IGS Workshop, University of Berne, Berne, pp. 351–360, 1993.